Jour. Korean Earth Science Society, Vol. 23, No. 1, p. 1-14, January 2002

Landsat TM Based Land-cover Analysis of Cholwon (South Korea) and Wonsan (North Korea)

Moo-Young Song*, Jong-Oh Park, Kwang-Soo Shin and Young-Chul Yu

Department Geology, Chungnam National University, Daejeon, 305-764, Korea

Abstract: The land-cover of two regions of South and North Korea included in one Landsat TM scene was investigated by comparing different seasons and different band data over the multiple land-cover types. The relationships between the intensities of two bands in the 2-D plot are mainly linear in band2 versus band1 and band3 versus band1, polygonal sporadic in band5 versus band1 and band7 versus band1, and almost tri-polarized in band4 versus band3. The 2-D plot of band4/band3 shows the best capability to discriminate different main land-cover such as water, vegetation and dry soil. Some discriminations are not clear between city and dry field, or mountain and plain field in the scene of September. The digital number data of band4 from vegetated zones show stronger reflectance in September rather than April, while other band values tend to be lager in April than in September over each land-cover. NDVI presents high value in both regions in September. However the image of Wonsan area in April suggests weak vigor of vegetation in comparison with Cholwon area. Band ratios are very effective in eliminating the influence of the complex topography. The proper pairing of the band ratio improved the discrimination capability of the land-cover; band5/band2 for dry soil, band4/band3 for vegetation and band1/band7 for the water. The RGB combination of the three band ratio pairs showed the best results in the discrimination of the land-cover of Wonsan, Cholwon and even the Demilitarized Zone.

Key words: land-cover, discrimination, multispectra, band ratio, vegetation

INTRODUCTION

Satellite remote sensing has become the useful strategy for the survey over the non-accessible area because of simultaneity, broad surface, repeatability, and possibility of thematic discrimination. Especially remote sensing surveys were successful over the plain field for the vegetation, harvest, and even for the natural resources (Grantz and Gentle, 1982; Pech *et al.*, 1986; Knick *et al.*, 1997; Vincent, 1997).

The Korean Demilitarized Zone (DMZ) is located in the middle part of the Korean peninsula which has the complicated surface morphology, and most of the homogeneous surface unit are small scale less than the Landsat image pixel size (30×30 m). Because of the military tension between South and North Korea, nobody could approach the region for the environmental or geographical research.

Our study regions, Wonsan and Cholwon are located in North and South Korea respectively, with the direct distance 110 Km, divided by DMZ and mountain range. Wonsan is a harbor city on the East Sea while Cholwon is located in the inner-land area. The two zones are connected as the Chugaryung Rift Zone which runs from Wonsan via Cholwon through Seoul and the southbound.

Our research purpose is to analyze comparatively the Landsat TM data with different seasons and seven different spectral bands over two regions for the land-cover characteristic identification. We compare the digital value of each pixel representing the reflectance of the block area of 30 m×30 m. We investigate the difference of the digital value of the pixel according to the land-cover objects, and their variance between different seasons. The intent of this paper is to get the proper interpretation technique for the environmental status when the spatial resolution become improved in a near future, probably up to 4 m (Dykstra, 1996).

Environmental monitoring will support the urban planning in the new territory development for the

*E-mail: mysong@cnu.ac.kr

reunification of Korea, and the vegetation evaluation around the DMZ. The extensive area including Cholwon and DMZ is the relatively flat surface in the central part of the Korean peninsula and has the possibility of developing center in Korea. Wonsan is the most important coastal city in North Korea. Environmental monitoring in such kind of area would be helpful for territory management or infrastructure development (Gumbricht *et al.*, 1996; Su *et al.*, 1992).

Here we investigate the real values of the image pixels, their representatives, the distribution characteristics concerning to the land-cover and the change between the different seasons through the direct statistic procedure (Robinove, 1982; Singh, 1989; Shimabukuro and James, 1991). Our favorable research result might be expected to analyze the vegetation cover in future (Pilon *et al.*, 1988; Narumaloni *et al.*, 1997), and it can provide the chance to understand the environmental situation more correctly.

GEOGRAPHICAL SETTING

Wonsan and Cholwon belong to the same Landsat TM scene (path 116 and row 33) in the middle east region of the Korean Peninsula, and located around N 39 10, E 127 30 and N 38 10, E 127 15 respectively (Fig. 1). Being divided by the mountain range which runs northeast with the summit height of 1500 m, Wonsan city is located on the east coast of North Korea as the most important city, and Cholwon, once a capital city of an ancient short-time dynasty, is located in the central part of the Peninsula, splitted into North Korea, DMZ and South Korea. The cited Cholwon in this study is a part of Cholwon belonging to South Korea just south of DMZ with 4 km width and 250 km length stretched in East-West. The DMZ area is absolutely inaccessible zone, and the expanded both sides with several kilometers may be considered to be limited from the general human activity because of the military alertness or protection.

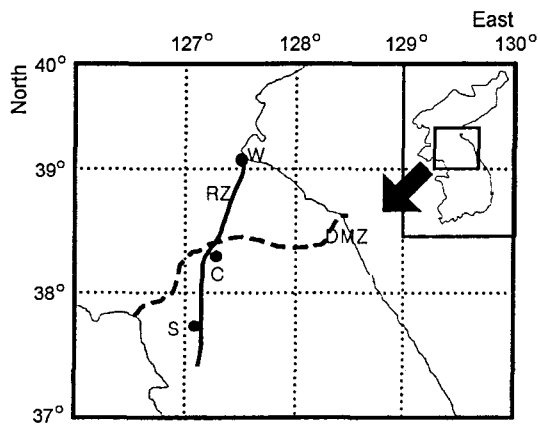

Fig. 1. Index map of the study area. DMZ divide Wonsan (North Korea) and Cholwon and Seoul (South Korea). Wonsan, Cholwon and Seoul are located on the lineament of Chugaryung Rift Zone (RZ).

The geology of this region is mostly composed of the Precambrian gneiss and Mesozoic granite. A great lineament is detected along the linear pattern from Wonsan through Cholwon even up to Seoul, and especially the segment from Wonsan to Cholwon is called as Chugaryung Rift Zone, which is composed of the Pleistocene lava flow and the Cretaceous tuffstone. The plain area around Cholwon is the Pleistocene basalt with the layer thickness of 50 m to 100 m. Hantan River flows along the boundary between basalt and granite or in the middle of basalt plain, and forms a narrow gorge (30 m width) with the cliff height of 25 m to 35 m.

This study region shows the annual average precipitation about 1,100 ~ 1,600 mm. The annual average temperature is 8 ~ 11°C, but the inner region shows the larger annual difference than the coastal region. Cholwon is known as the coldest area in South Korea with around −25°C at mid-winter because of the cold air mass, funneled through the Rift valley from the North, fanning out into the Cholwon plain area.

The seasons our Landsat image data were acquired are spring (April 5) and autumn (Sep. 12). The date, April 5 is about 50 days before the rice-planting season in the paddy field. There is not yet much water in the paddy field in this period. On

the mountains trees do not yet sprout also. Therefore we can expect the least vegetation on the land without snow. On the other hand the date, Sep. 12 is about 30 days before the harvest season from the paddy field and also before the turning-red of the deciduous tree. Therefore through the image comparison between these two seasons we could investigate the vegetation influence in maximum.

Moreover, the two dates of data acquisition keep the similar sunshine condition, because of the sun-synchronous orbit of Landsat 5, and the dates of 15 days after the vernal equinox and 10 days before the autumnal equinox respectively. In the two image scenes, the sun sustains 142.5 degree in orientation (N clockwise) and 31.2 degree in altitude because the satellite crosses the region (N 39) at 9 : 35 AM.

ANALYSIS PROCEDURE

Our satellite image data are the Landsat TM (* The US government retains ownership of the data. EOSAT and NASDAC supported us in acquiring the satellite data at marginal cost) dated April 5, '94 and Sep. 12, '94, over the region of the track of Landsat 4, 5 with path 116 and row 33, centered of N38.52, E127.11. The cover area is 180 km×180 km with the oblique direction S15W. The coordinates of four corners are N39.46, E126.22 (NW), N39.26, E128.30 (NE), N38.16, E126.02 (SW) and N37.56, E128.06 (SE). The time difference for the data acquisition between the NW corner starting point and the SE final point of the scene is about 24 seconds. We suppose that during the period there was no great change in the environmental condition over the area or in the atmospheric layers' physical condition.

The digital satellite data used to be reserved as CCT, CD-ROM, 8 mm or 4 mm cartridge tapes. Our Landsat TM data were composed of 7 header files and 7 data files according to the bands of the electromagnetic wavelength. The Thematic Mapper spectral bands in the increasing order of the wavelength are Band1: blue (0.45 ~ 0.52 m), Band2: green (0.52 ~ 0.60 m), Band3: red (0.63 ~ 0.69 m), Band4: near infrared (0.76 ~ 0.90 m), Band5: mid infrared (1.55 ~ 1.75 m), Band7: mid infrared (2.08 ~ 2.35 m), and Band6: thermal infrared (10.4 ~ 12.5 m). The order reverse of Band7 was due to the later addition to the original system design process of the satellite Landsat 4. Because of the importance of the wavelength, we keep the wavelength order in this presentation for the comparison of bands.

The header file can be read through the common Notepad and we get the information about the data file format. The main information in the header file are description of band number over the region, samples, lines, bands, header offset, file type, data type, interleave, byte order, and band names. We have in this study the data variables; 7020 for samples, 5965 for lines, integer for data type, BSQ (band sequential) for interleave. The header file information is a prerequisite to open the data file.

The data processing packages are known as the names: PCI, ERDAS, ENVI, etc. We used the ENVI version 2.6 in this study, which is developed relatively recent and very powerful, being arranged by the Interactive Data Language (IDL: trademark of Research System Inc.).

After the input of data using ENVI software package, we carried out the usual digital data processing (Table 1); mainly linking, X and Y profiles, cursor location/value, region of interest, 2-D scatter plot, overlay, annotation of File pulldown menu, statistics of ROI of Basic Tools pulldown menu, tape utilities of Utilities, NDVI, band ratio of Transforms, Isodata unsupervised classification of Classification pulldown menu (refer to ENVI Users guide V. 2.6).

The processing procedure is delineated on the flow chart of Fig. 2. The preprocessing on the geometric correction was carried out by the image data supplier (NASDAC), and for the other processing ENVI was used with our ground control point (GCP) for multispectral data collection on the region of interest (ROI), inter-band relationship, and land-cover classification. The detail description of the data pro-

Table 1. Standard deviation of DN read in Wonsan area by pixel (30) and ROI.

LANDCOVER	Band 1	Band 2	Band 3	Band 4	Band 5	Band 7	Band 6	
As-sea	1.207	0.794	0.907	0.817	0.845	1.048	0.507	
Ab-beach	5.425	3.752	6.677	7.2	10.579	10.619	1.751	
Ap-field	1.507	0.774	1.194	4.683	4.521	2.254	0.817	
Ac-city	3.683	2.033	3.234	4.213	5.155	2.7	2.078	
Ams-mt s	1.431	1.264	1.478	8.261	5.771	2.159	2.861	
Amd-mt d	1.724	0.728	1.015	3.411	3.308	1.617	0.73	Reading in 30 points
Ss	1.408	1.186	0.794	0.507	0.907	1.017	0.817	
Sb	6.222	4.92	7.531	5.307	14.307	10.104	3.231	
Sc	2.1	1.567	2.912	2.318	4.169	2.468	1.956	
Sp	1.708	1.098	1.143	0.897	6.381	4.818	1.732	
Sms	2.491	1.424	2.608	2.135	7.737	5.275	1.855	
Smd	1.455	1.04	1.857	2.712	5.833	3.418	1.442	
As-sea	1.432	0.769	1.398	0.556	1.035	0.917		
Ab-beach	10.662	9.662	13.611	10.967	23.673	17.049		
As-field	3.57	2.54	4.642	4.834	16.859	11.779		Reading in ROI
As-city	5.394	2.233	3.775	3.4	5.769	3.8		
Ams-mt s	3.968	3.12	5.971	5.072	13.511	8.447		
Amd-mt d	6.441	2.115	3.718	4.912	13.427	7.456		

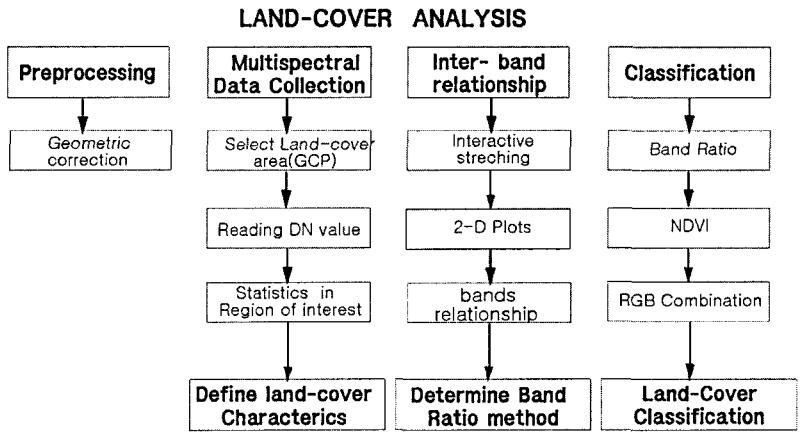

Fig. 2. Flow chart on the data processing procedure with ENVI for land-cover analysis.

cessing is out of our research here, but the readers may refer to the references (Markham *et al.*, 1985; Raitala and Lenpinen, 1985; Canters, 1997; Vincent, 1997).

Our main processing is the followings; 1) We limited the Landsat TM image to the Path 116-row 33, dated on April 5 and Sep. 12, 1994. Our study was focused at Cholwon and Wonsan region. 2) In each region we selected the main land-cover units; mountain, sunny side, mountain shadow side, plain field, cities, and water for Cholwon region, and mountain sunny side, mountain shadow side, plain field, Wonsan city, coastal beach, and sea for Wonsan region. 3) We read the Digital Number (DN) of the 30 pixels of the reliable land-cover for every unit using the command cursor location/value with zoom window. For the DN values we obtained the average and standard deviation. We considered them as the basic information to manipulate the processing. 4) In order to compare the DN value for the land-cover unit, we carried out the region of interest (ROI) to collect the statistics of the asking polygon area. Especially, we will discuss the difference of standard deviation of DN values between 30 pixels reading and ROI statistics. 5) Our interest is concentrated to the variation of DN value

according to the land-cover, season, and the spectral wavelength. Then we analyze the DN distribution on the different bands. 6) We compared the bands pair using 2-D plot in order to find what pair can show the most separable information. We will discuss the efficiency of the 2-D plot characteristics. 7) For the visual discrimination of the land-cover, we tried several RGB combinations indicating more clearly for certain land-cover characteristics. 8) Following the automatic process, we carried out the unsupervised classification in two dif- ferent cases; for the band4 and the Metafile composed of all 7 bands. The classification was into 5 division. 9) We calculated the vegetation index, specially, Normalized Difference Vegetation Index (NDVI), and the results were visualized through RGB combination with band7 and band1 for red and blue, respectively. 10). After the combination of 3 band ratios for the sensitive main land-cover difference was selecting through the trial and error, we calculate band ratios for band5/band2, band4/band3, and band1/band7. 11). We combined the three ratios for RGB combination for the visual presentation, and discussed the environmental characteristics in Wonsan, Cholwon and DMZ.

RESULTS AND DISCUSSION

Reflectance Intensity Distribution

For the understanding of the outline and main trend of the reflectance distribution, we read the DN value of pixels over the important land-cover area because the DN is the basic response of the physical characteristics of the land-cover (Knick *et al.*, 1997). The analysis of the data is usually done on the basis of the digital levels. The levels are related by a linear calibration to the intensity of reflected radiant energy. We analyze the DN data directly without the conversion for the reflectance value as Robinove (1982).

Figure 3 and Fig. 4 show the pattern of the DN value of each land-cover according to the bands. The X axis value indicates the band number, except that 6 indicates band7 and 7 means band6 because of the order of wavelength. The digital value in Y axis indicate the average DN of the 30 pixels sepa-

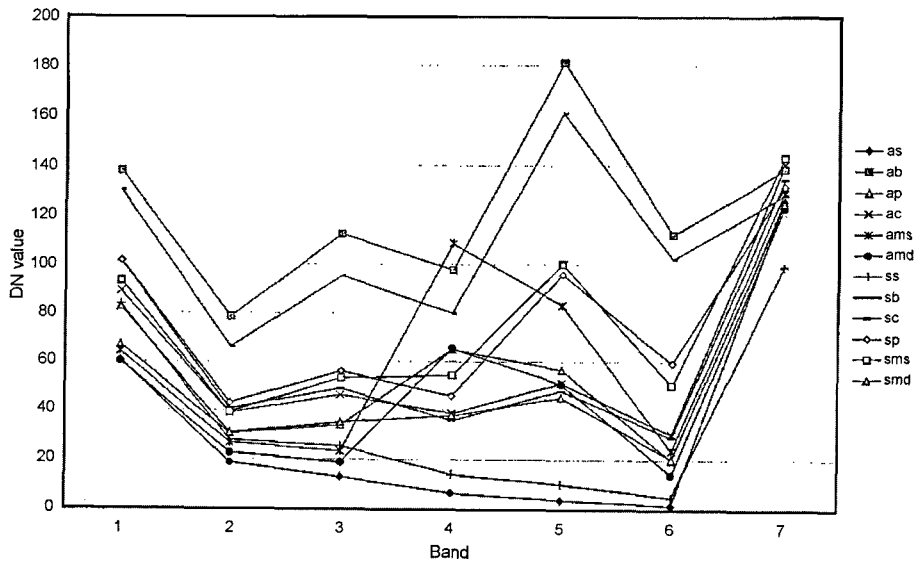

Fig. 3. Digital Number (DN) distribution over the main land-cover in the Wonsan region according to the wavelength sequence (6 means Band7 and 7 means Band6). AS: Autumn sea, AB: Autumn beach, AC: Autumn Wonsan city, AP: Autumn plain field, AMS: Autumn mountain sunny side, AMD: Autumn mountain shadow side, SS: Spring sea, SB: Spring beach, SC: Spring Wonsan city, SP: Spring plain field, SMS: Spring mountain sunny side, and SMD: Spring mountain shadow side.

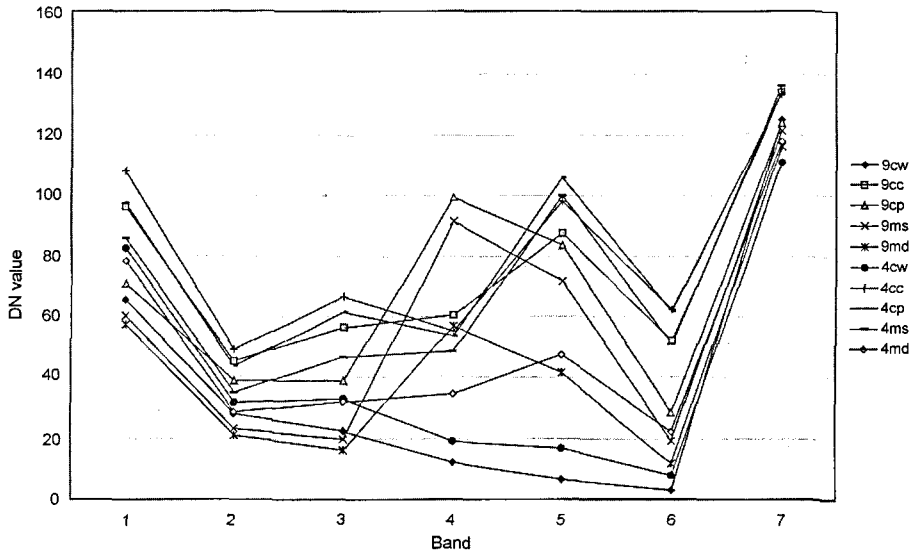

Fig. 4. Digital Number (DN) distribution over the main land-cover in the Cholwon region. 9CW: Autumn water reservoir, 9CC: Autumn small cities, 9CP: Autumn plain field, 9MS: Autumn mountain sunny side, 9MD: Autumn mountain shadow side, 4CW: Spring water reservoir, 4CC: Spring small cities, 4CP: Spring plain field, 4MS: Spring mountain sunny side, and 4MD: Spring mountain shadow. The seasonal variance is detected very strong in the Band4.

rately read from each land-cover image through the enlarged zoom window. Because the land-cover area was not always large enough to cover the homogeneous land-cover characteristics, some pixels may contain several land-cover characteristics and show impurity. Zoom window provided the effective tool to identify the reasonable pixel for each land-cover, and the cursor location/value extracts the pixel value. Except this reading using cursor location/value, it is possible to get the statistics of DN through Region of Interest (ROI), not the separate independent pixel but the whole group of the land-cover. We found that the difference between the two average values was less than 0.5, and the standard deviation was very large in Region of Interest. It seems to be originated that the separate pixel reading can be extracted in the similar condition, while the Region of Interest may include the impure land-cover characteristics too. Table 1 shows the standard deviation of the DN in Wonsan area for the 2 cases; each pixel reading (30 pixels) and ROI reading (>10000 pixels). Especially, the large standard deviation can be detected in a small size or complex land-covers such as beach (ab), mountains (ams, amd), which are compared with the sea cover (as) of small standard deviation.

In Fig. 3, we compare the DN of the pixels of different land-covers in Wonsan region of two seasons; autumn (as through amd) and spring (ss through smd). The legend indicates the land-cover characteristics; sea (as, ss), beach (ab, sb), plain field (ap, sp), Wonsan city (ac, sc), mountain sunny side (ams, sms) and mountain shadow side (amd, smd). The X axis indicates the Band number except 6 means Band7 and 7 means Band6 according to the wavelength order. Band6 (7) takes the pixel cover area up to 120 m×120 m, comparing with the others 30 m×30 m. The DN value of Band6 is not so discernible for the land-cover.

Here we can find several trends of the DN distribution: 1). Beach has the highest value, the seawater the lowest, and the others the intermediate. 2). The vegetation areas (ap, ams, amd) show the extra high value in Band4 in autumn in comparison to spring. 3). Autumn beach shows the larger value than spring, but over the sea autumn value is lower

than spring. 4). If we try to find the indicating band pair for the land-cover characteristics, we can choose that band5/band2 is for beach, band1/band7 (6) for water, and band4/band3 for the vegetation area. 5). The ratio of the DN of sunny side to the shadow side is not constant in different bands, but show the similar rates in the longer wavebands.

The opposite trend of the seasonal difference between beach (autumn > spring) and seawater (spring > autumn) makes us confused, but in part there is the possibility that the spring sunshine is a little stronger than the autumn, and beachs dryness effect in autumn may surpass the sunshine effect of spring. The vegetation effect seems give the higher value in Band4 and a small increase in Band5. This trend suggests how to extract the vegetation index, and how to discriminate the vegetation area from the others.

Figure 4 is the version of Cholwon, South Korea, located near DMZ in central part of the Korean peninsula. Here, the legend shows the autumn scene (9cw through 9md) and the spring scene (4cw through 4md), and water (cw), small cities (cc), plain field (cp), mountain sunny side (ms), and mountain shadow side (md). In this region there is no coastal beach and seawater, but small water reservoirs for the agriculture. We can find here also several trends of the DN distribution: 1). Water reservoir shows the low DN, but in the visible ray ranges (bands 1, 2, and 3), autumn mountains (flourishing vegetation) take lower value than water. 2). Like Wonsan, the high vegetation area (mountains and plain field) increases the DN of Band4 in autumn in comparison with spring. 3). Small cities also show small increase of DN of band4 in autumn, which is different in Wonsan city. 4). The sensitive band ratio pairs are obvious for the land-covers; band5/band2 for spring plain field and mountain sunny side, band4/band3 for autumn plain field and mountains, and band1/band7 for the waters.

In Fig. 3 and Fig. 4, we found the following phenomena: 1). The flourishing vegetation makes change the DN value decreasing in visible ray bands (1, 2, 3), but strongly increasing in near infra red (band4). The low value in visible ray suggests the effect of the moisture of the forest vegetation. 2). Small cities of the increasing DN in the band4 suggest that there are less concrete buildings and more trees in small cities of Cholwon region comparing with the larger Wonsan city. 3). From the DN distribution pattern we can choose the effective band ratio pairs to discriminate the land-cover characteristics. 4). Dry soil shows the high DN value in all bands, water shows the low, especially in the increasing wavelength, and the other common land-cover the intermediate value with variation of vegetation.

Inter-band Relationship

We compared the relationships between the every band pairs in 2-D plots. Except the band6 of the thermal infra red, we have 6 bands for the possible pairs and we can obtain the 15 combination. Among them we selected the main band pairs presented as Fig. 5. This figure is the 2 dimension relationship of the Landsat TM dated on Sep. 12, 1994, for Wonsan. From the top left they are the followings for Y axis/X axis; band2/band1 (A), band3/band1 (B), band4/band1 (C), band5/band1 (D), band5/band3 (E), and band7/band1 (F). The patterns can be divided into three categories; A and B are almost linear, C spreadings into the tripod, last three polygonal pattern.

In the first and the third categories it is difficult to discriminate the different land-covers, but in the second category of the band4/band1 2-D plot we can find the different land-cover through the pixel dancing or the ROI drawing in the ENVI operation. In the plot of band4/band1, the bottom corner is identified to the water, the middle right corner (greatest value of band1) to the dry soil, and the top corner (greatest value of band4) to the vegetation. In fact the band4/band3 is better than band4/band1.

Figure 6 shows the band pair (band4/band3) relation for Cholwon and Wonsan in different seasons. The upper two (A and B) are for the image of

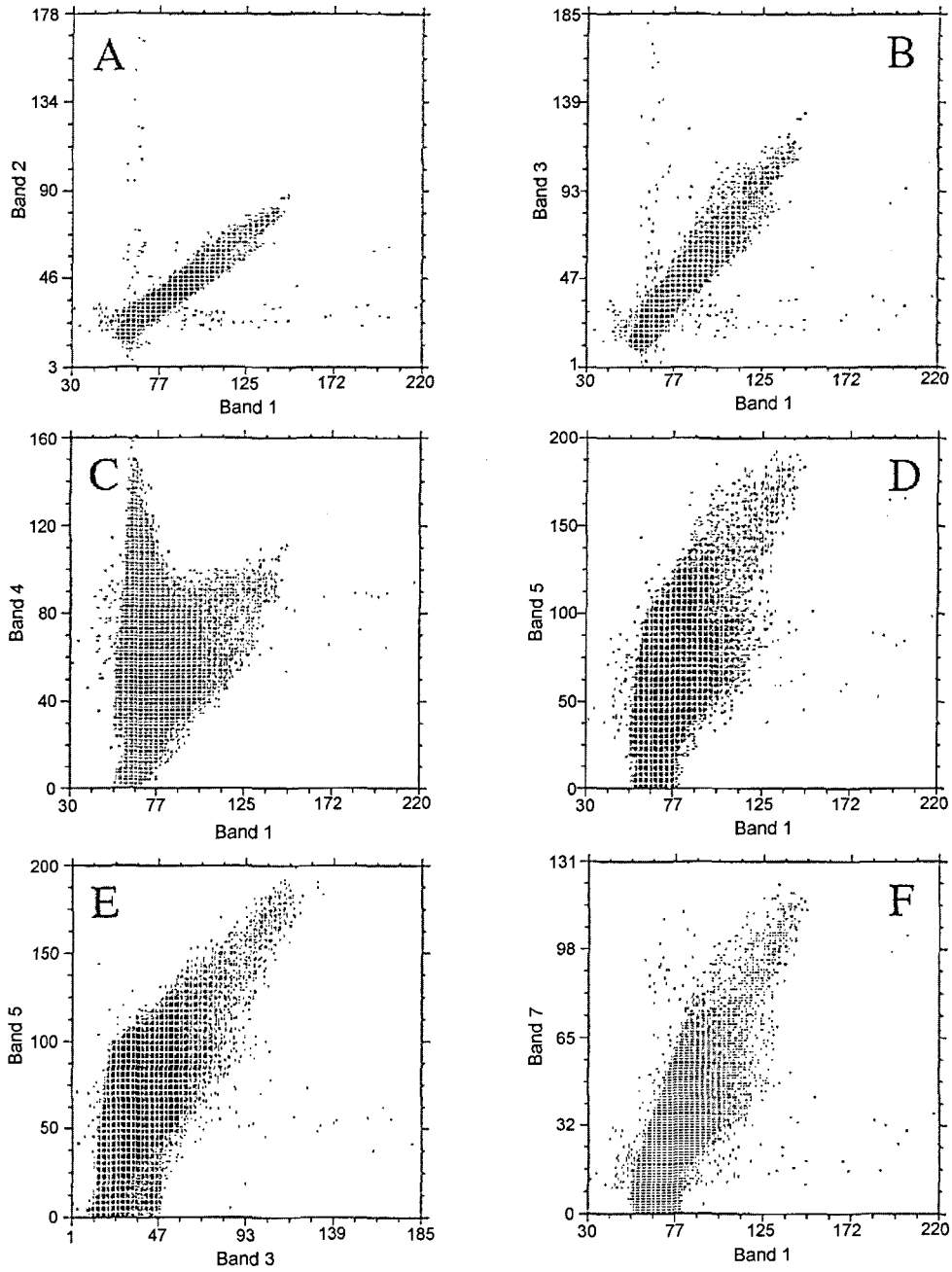

Fig. 5. 2-D scatter plots of DN values of 400×400 pixels of Wonsan region. Note that A and B are linear pattern and D, E, and F are polygon, but b4/b1(C) shows the tripod.

April 5, 1994 for Cholwon and Wonsan respectively, and C and D for Sep. 12, 1994. For all the two rows the left are for Cholwon and the right for Wonsan. Because the computer controlled the axis range automatically the maximum value of the each axis is not constant.

Considering this factor we can easily figure out the seasonal change in the tripod type. In the upper two plots there are weak tripod pattern, but in the bottom two the tripod type are reinforced. It sug-

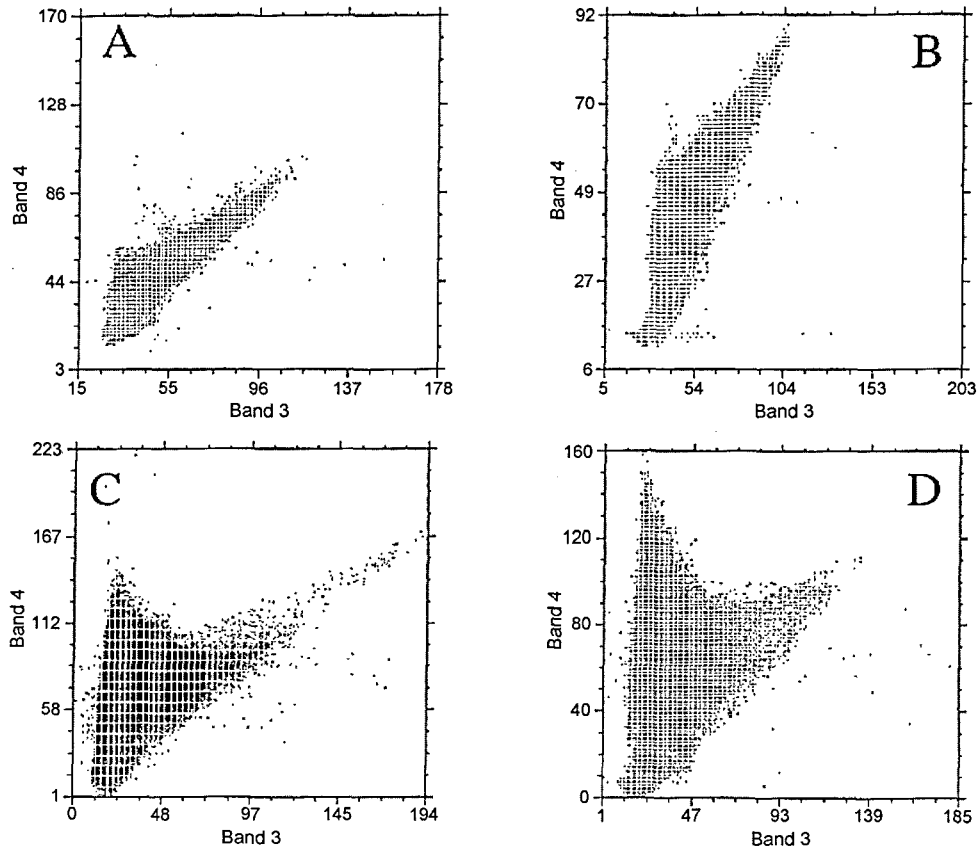

Fig. 6. 2-D scatter plots of DN values of 400 × 400 pixels in b4/b3 for Y/X axes. A and B are for Cholwon and Wonsan in April, and C and D for Cholwon and Wonsan in September. Note that the tripod is weak in the above two graphs in April, but strong in September. The tripod corner point coincides with dry soil (middle right), heavy vegetation (top), and water (bottom).

gests the vegetation effect in the September. The vegetation land-cover can be discriminated easily with this band4/band3 plot. As we described above the three corners of the tripod type pattern are identified to the three main land-covers; the top-left corner to vegetation of forest, the middle-right corner to the dry soils, and the bottom corner to the water, whether sea, river or reservoir. The closer to the central point of the plot, the more confusing for the identification of the land-covers.

Classification with NDVI and Band Ratio

Since the vegetation quantification by Rouse, 1973 with bands 7 and 5 of Landsat MSS, the vegetation index was often cited for the assessment of the vegetation such as forest, agriculture, even harvest evaluation in terms of the VI, NDVI or TVI (Lillesand and Kiefer, 1994). We followed the NDVI for the comparison of the vegetation differences between the two regions and the two seasons. Usually NDVI is defined as the difference of the DN of band3 from band4 divided by the sum of the DN values of the two bands.

The NDVI result was visualized in RGB combination with band7 for red, band1 for blue, and NDVI for green as Fig. 7. As we mentioned above, since the great DN in band4 was obvious, the difference of the DN between band4 and band3, the ratio band4/band3, and the NDVI can be indicators for the vegetation quantity. The choice of the band1 and band7 for the RGB combination pair was in free trial because they are farther in the

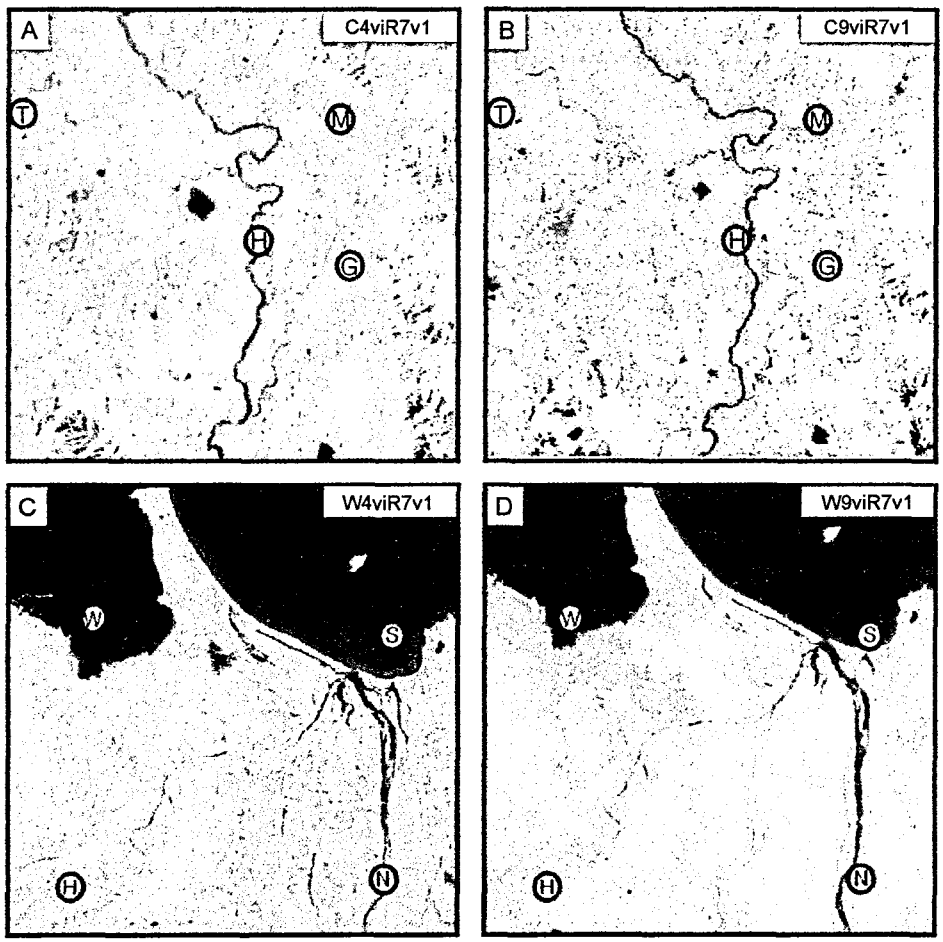

Fig. 7. RGB combination with band7, NDVI, and band1. A and C are for spring images and B and D for autumn, indicating the upper for Cholwon area and the bottom for Wonsan area. The greenish tonal difference between two regions suggests the weak forest in Wonsan mountains and the late harvest in Wonsan paddy field.

wavelength from band3 and band4.

Figure 7 shows the RGB false color composite for Cholwon (top two) and Wonsan (bottom two) in different seasons; left two for April, and right two for September. Cholwon region was studied in detail during last several years by our team and some geologists (Shin, 1998), but we have been limited from the information about Wonsan because of the communication interrupt since 1948.

All images point out the soil for pink to red, the water cover (river, reservoir and sea) for blue, and forest or cultivated vegetation for green. In the images of April 5, 94, the pinkish surface largely expanded because the spring sprouting was not yet prosperous. In Cholwon, the plain area near Hantan River is of basalt floor originated from the Quarternary volcanic eruption in the Chugaryung Rift Zone. The other pink zone is the farming field consisting of the erosion surface of granite or gneiss.

In Wonsan, April, all the plain fields and some part of the mountains show pinkish purple and it suggests that the mountains around Wonsan have the weak density of the vegetation comparing with Cholwon area, and the plain field was not cultivated during the winter season.

In the images of September, green surface becomes expanded up to all mountains and the plain field except the city area. The season of September 12 is

close to the ripening of rice, becoming yellowish from green. The harvest season seems to be a little bit earlier in Cholwon than in Wonsan because of the higher altitude with continental climate in Cholwon. The coastal beach and the airport runway can be easily identified in the September Wonsan image, but the highway is not clear, maybe less than in several false color RGB combinations based on the original bands. The common false color composites are omitted in this presentation.

As we have already described above, the main land-covers are sensitive separately to the special band ratios. After some trial and error on the base of the DN distribution pattern, we decided the best

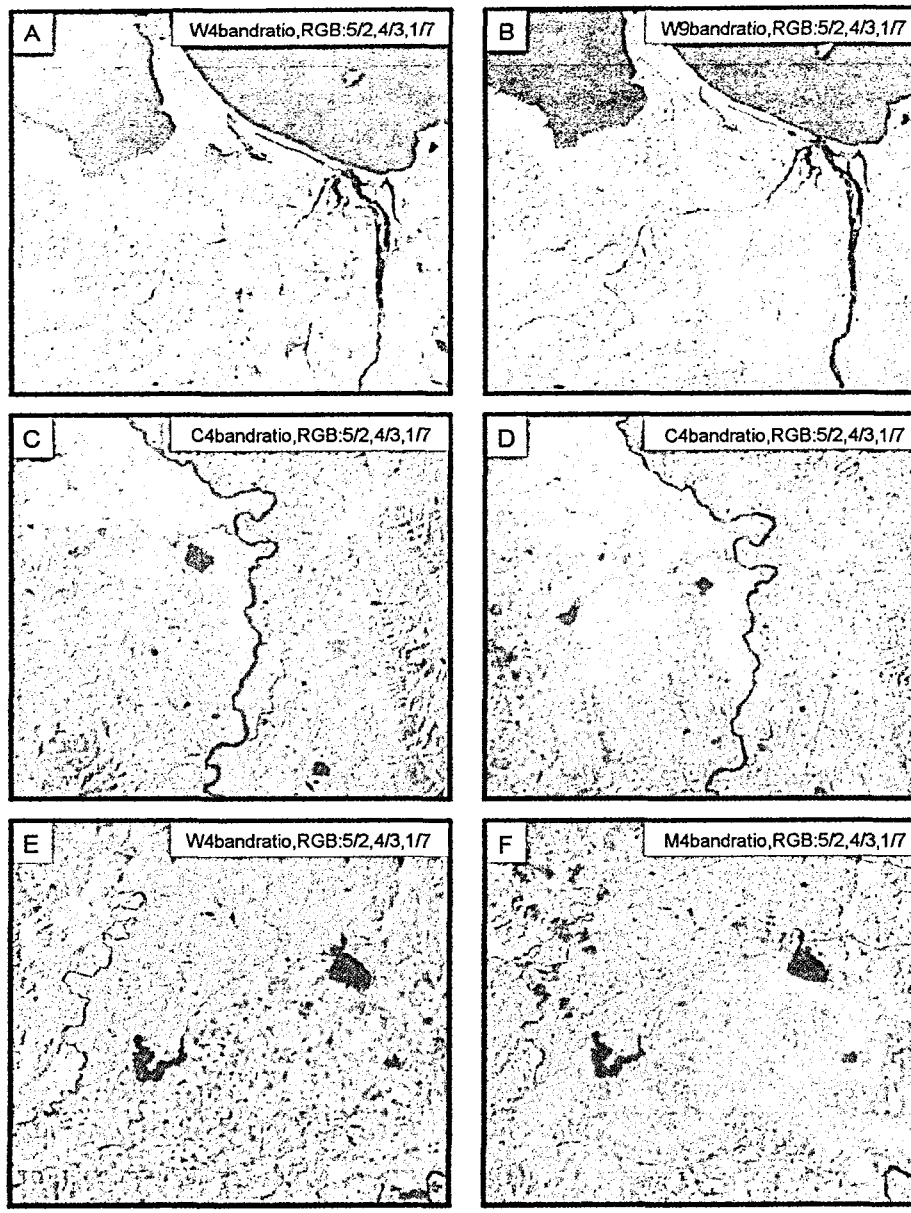

Fig. 8. Band ratios and RGB combinations. For dry soil the band ratio b5/b2 is chosen, for vegetation b4/b3, and for water b1/b7. These three band ratios are combined for RGB in sequence. The upper two figures are for Wonsan, the middle for Cholwon, and the bottom for DMZ. The lefts are for spring and rights for autumn.

band ratios (Crist and Cicone, 1984; Drury, 1993); band5/band2 for dry soils, band4/band3 for vegetation, and band1/band7 for water (Lillesand and Kiefer, 1994). The three band ratio pairs are chosen for the RGB combination like Fig. 8, which show the results for the region of Wonsan (top two), Cholwon (middle two), and Demilitarized Zone near Cholwon (bottom two). All the left images are April and all the right September. In all the images the water cover are most prominent as blue.

In Wonsan's image of April we can interpret that the relatively small surface area keeps the evergreen like conifers and the most expanded surface has no much vegetation or deciduous forest. All the soil-covered zones show similarly the brownish tone whatever the land-cover is; beach, highway, field, and mountains. In the September images, the soil-covered zones are divided into dry soil or highway for red and the paddy field for dark green. We can detect the airport runway and riverside sand zone also. In the mountains pale green area is enlarged in comparison to the April image. But the red spots scattered around the pale green mountain area suggest the weak vegetation density in the mountain forest. If the deciduous tree was the main plat, September image could not show the reddish response. The Wonsan's brown tone suggests the large city which has large building and their shadow, comparing to the small cities in Cholwon region with red tone.

In Cholwon image of April, we can read easily the mountains conifers such as pine trees which were observed by us when we survey to verify the more than 60% of mountains vegetation of pine tree. The pale brown area occupies the soils, or the weathered shrub and grass, because of the non-agricultural season. In September image we can see the small cities of red color and the new extended road between them in the middle part of the right half. Some large red zone might be the vinyl house for the forced vegetables. The scattered red spot in the plain field of the left side of Hantan River seems to be the dried paddy field for the coming harvest or the already harvested field. We can concentrate here that the mountain area show the green or pale green but not the red spot among them, which is different from Wonsan area.

In DMZ image of April, except the reservoirs and small rivers, most surface area shows the yellowish brown tone suggesting the weathered shrub or deciduous forest. This region is the plain topography and is presumed no many conifers differently from the mountain area. In this image it is difficult to outline the DMZ from the Northern Limit and the Southern Limit. On the other hand, the September image indicates the boundary and the homogeneity of land-cover of the DMZ. We can find out the Northern Limit and the Southern Limit (broad and clear) and even the trails of the military monitoring or sentinels. The homogeneous yellowish green tone can be interpreted as the result of the ecological balance in the DMZ due to the non-access during last 50 years. Some patches of the dark blue and the brown tone are the effect of the scattered clouds; the shadow and the cloud itself, separately. The cloud itself shows the high intensity in the visible ray and near infra red, but very weak in the thermal infra red (Band6). On the contrary the shadow of the cloud shows the low intensity in the visible and near infra red, and relatively high in the thermal infra red.

In the comparing procedure of the results of NDVI and band ratio combination, we found that the original bands DN values became the focus for the analysis, and the RGB combinations of the original bands provided us with the clue to the analysis orientation, even though the RGB combinations are omitted in this presentation due to the common usage by many researchers.

In this study we have not yet found the better result with the supervised and unsupervised classification, maybe partly because of the lack of the training sets for the supervised (Joria and Jorgenson, 1996), and of the automatic process for the unsupervised classification. This question remains for the future.

Heaton, J. in the Department of Geosciences, Oregon State University, for their discussion and help in data transfer and management when the first author visited OSU.

REFERENCES

Canters, F., 1977, Evaluating the uncertainty of area estimates derived from Fuzzy Land-cover classification. Photogrammetric Engineering and Remote Sensing, 63(4), 403–414, A2.

Crist, E.P. and Cicone, R.C., 1984, A Physically-Based Transformation of Thematic Mapper Data- The TM Tasseled Cap. IEEE Transactions Geoscience and Remote Sensing, 22(3), 256–263.

DA., 1993, Image Interpretation in Geology. 2nd ed., Chapman & Hall, p. 283.

Dykstra, J., 1996, Four-meter resolution multispectral satellite data and its implications for crop monitering and distribution mapping. SPIE 1966 annual meeting, Space Imaging EOSAT, 303-254-2103.

Grantz, R.D. and Gentle, M.R., 1982, The relationships between reflectance in the Landsat wavebands and the composition of an Australian semi-arid shrub rangeland. Photogrammetric Engineering and Remote Sensing, 48(11), 1721–1730.

Gumbricht, T., McCarthy, J., and Mahlander, C., 1996, Digital Interpretation and management of land-cover a case of Cyprus. Ecological Engineering, 6, 273–279.

Haack, B., 1987, An assessment of Landsat MSS and TM data for urban and near-urban Land-cover digital classification. Remote Sensing of Environment, 21, 201–213.

Joria, P.E. and Jorgenson, J.C., 1996, Comparison of Three Method for Mapping Tundra with Landsat Digital Data. Photogrammetric Engineering and Remote Sensing, 62(2), 163–169.

Knick, S.T., Rotenberry, J.T., and Zariello, T.J., 1997, Supervised classification of Landsat Thematic Mapper Imagery in a semi-arid range-land by non-parametric Discriminant Analysis. Photogrammetric Engineering and Remote Sensing, 63(1), 79–86.

Lillesand, T.M. and Kiefer, R.W., 1994, Remote Sensing and Image Interpretation. 3rd ed., John Wiley and Sons, p. 750.

Markham, B. and Barker, J.L., 1985, Spectral characteristics of the Landsat Thematic Mapper sensors. International Journal of Remote Sensing, 6(5), 697–716.

Narumaloni, S., Jensen, J.R., Althausen, J.D., Barkhalters, S., and Mackey Jr., H.E., 1977, Aquatic Macrophyte Modelling using GIS and logistic multiple regression. Photogrammetric Engineering and Remote Sensing, 63(1), 41–49.

Pech, R.P., Davis, A.W., and Lamacraft, R.R., 1986, Calibration of Landsat data for sparsely vegetated semi-arid range lands. International Journal of Remote Sensing, 7(12), 1729–1750.

Pilon, P.G., Howarth, P.J., and Bullock, R.A., 1988, An Enhanced classification approach to change detection in semi-arid environments. Photogrammetric Engineering and Remote Sensing, 54(12), 1709–1716.

Raitala, J. and Lenpinen, J., 1985, A Landsat study of the aquatic vegetation of the Lake Luodonjarvi Reservoir, Western Finland. Aquatic Botany, 21, 325–346.

Robinove, C.J., 1982, Computation with physical values from Landsat Digital data. Photogrammetric Engineering and Remote Sensing, 48(5), 781–784.

Shimabukuro, Y.E. and James, A.S., 1991, The Least-Squares mixing model to generate Fraction images derived from remote sensing multi-spectral data. IEEE Transactions Geoscience and Remote Sensing, 29(1), 16–20.

Singh, A., 1989, Digital change detection techniques using remotely-sensed data. International Journal of Remote Sensing, 10(6), 989–1003.

Shin, Kwang-Soo, 1998, The application of Landsat TM data to Geological Interpretation and Land-cover Classification in Cholwon. Master thesis of Chungnam National University, p. 89.

Su, Y., Chen, S., Zhao, Y., and Chen, L., 1992, Monitoring Urban Development of Hangzhou City by using multi-temporal TM data. GIS, 2, 8–13.

Vincent, R.K., 1997, Fundamentals of Geological and Environmental Remote Sensing. Prentice Hall, p. 366.

Manuscript received October 8, 2001
Revised manuscript received November 1, 2001
Manuscript accepted November 20, 2001